05,08

Evaluation of Dzyaloshinskii–Moriya interaction in metallic nanoheterostructures: methodology and experiment

© A.V. Telegin[1], Zh.Zh. Namsaraev[2], V.A. Bessonova[1], V.A. Antonov[2], S.V. Batalov[1], A.V. Ognev[2,3]

[1] M.N. Mikheev Institute of Metal Physics, Ural Branch, Russian Academy of Sciences, Yekaterinburg, Russia
[2] Far Eastern Federal University, Vladivostok, Russia
[3] Federal State Budgetary Educational Institution of Higher Education Sakhalin State University, Yuzhno-Sakhalinsk, Russia

E-mail: telegin@imp.uran.ru

Received November 24, 2024
Revised December 4, 2024
Accepted December 4, 2024

A theoretical and experimental study of the weak antisymmetric Dzyaloshinskii–Moriya exchange interaction in multilayer metal nanostructures of the heavy metal/ferromagnet type is carried out. To assess the Dzyaloshinskii–Moriya interface interaction, methods for studying the dynamics of magnetic domains in a film, determining the magnitude of the current-induced field from the value of the external magnetic field in the plane of the film, and studying the magnetic domain nucleation field are considered. An experimental comparison of the methods is carried out and it is shown that for the Pt(4)/Co(0.7)/MgO(2 nm) nanostructure, yield similar estimates of the Dzyaloshinskii–Moriya interaction field, but the domain nucleation method is technically easier to implement and places fewer demands on the quality of the samples. This method is recommended for studying the evolution of the Dzyaloshinskii–Moriya interaction energy in thin-film nanostructures along with the widely used contactless method for estimating spin-wave dispersion anomalies.

Keywords: Dzyaloshinskii–Moriya interaction, nanostructures, current-induced dynamics, magnetic domains, Kerr microscopy, Spin-Hall effect.

DOI: 10.61011/PSS.2024.12.60216.323

1. Introduction

Topological spin structures, such as chiral domain walls (DWs) and skyrmions are considered as promising information media for future spintronics applications [1–3]. It is known that the electrical current may induce the motion of such spin structures, which makes them especially attractive for the promising memory devices and logic elements. The important parameter required to stabilize chiral spin structures is Dzyaloshinskii–Moriya interaction (DMI). DMI is anisotropic exchange interaction, causing orthogonal building of adjacent magnetic moments in the systems without the inversion center [4–7]. It occurs due to spin-orbit coupling which acts as a perturbation to localized spin states. If two adjacent spins $\mathbf{S}_i$ and $\mathbf{S}_j$ are present, DMI contributes to Hamiltonian locally with the first bilinear energy member described by the following expression:

$$\mathbf{E}_{\mathrm{DMI}} = \mathbf{D}_{ij}(\mathbf{S}_j \times \mathbf{S}_i), \qquad (1)$$

where $\mathbf{D}_{ij} = D_{ij}(\mathbf{r}_{ij} \times \mathbf{n})$ — local DMI vector in isotropic film described by its value D_{ij}, $\mathbf{r}_{ij}$ — single vector that connects to each other two adjacent magnetic nodes (atoms), and $\mathbf{n}$ — normal line directed along the disturbance of symmetry (in case of planar structures, normal line to the film plane).

The expression (1) is a part of the generalized exchange interaction, which relates value $\mathbf{D}_{ij}$ with isotropic Heisenberg exchange $\mathbf{J}_{ij}\mathbf{S}_i\mathbf{S}_j$, where J_{ij} — exchange constant. Contrary to the opposite collinear Heisenberg interaction, DMI promotes an orthogonal alignment of $\mathbf{S}_i$ and $\mathbf{S}_j$ with chirality imposed by sign $\mathbf{D}_{ij}$.

DMI concept was first proposed in 1950s for antiferromagnetics, such as α-Fe_2O_3, to explain the existence of weak ferromagnetism therein [4]. In subsequent decades other magnetic materials, such as spin glasses, orthoferrites, manganites or superconducting cuprates were studied for their noncollinear or spiral magnetism and DMI effect on magnetic state. In non-centrosymmetric crystals, such as MnSi, FeGe etc., it was shown that volume DMI results in appearance of skyrmion lattices and other exotic spin structures, which may be directly visualized at low temperature [8–10].

Quite recently the presence of strong DMI was demonstrated, localized in the interface between the layers in thin magnetic multilayer systems with perpendicular magnetic anisotropy (PMA) [11,12]. Interface DMI is important in the context of the systems comprising of a nanometer-thick FM film with PMA contacting with a layer of a heavy metal. In such system the interaction DMI arises due to the breaking of the inversion symmetry at the interface between

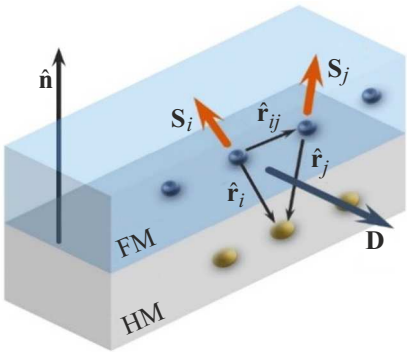

Figure 1. Schematic image of orientation of spins $\mathbf{S}_i$ and $\mathbf{S}_j$ in ferromagnetic (FM) layer which are built noncollinearly as a result of exchange interaction with atoms of the adjacent heavy metal (HM) layer. Direction of spin tilting direction is determined by orientation of the vector **D**, which is perpendicular to the plane formed by two atoms of FM layer and one atom of HM layer.

the two layers and large spin-orbit bond of heavy metal atoms, which mediate the interaction between the adjacent spins $\mathbf{S}_i$ and $\mathbf{S}_j$ of the ferromagnetic. The result of the DMI interface nature is reduction of the interaction value with the increase of the magnetic film thickness. If the symmetry breaking occurs only at the interface, and the planes or axes of symmetry are always perpendicular to the film plane, then, according to the Moriya rules, vector **D**, defined at the interface, must be perpendicular to the normal line of the film, as shown in Figure 1.

Taking into account the fact that ferromagnetic film is isotropic (i.e. has no specific dedicated directions), DMI vector is simplified to $\mathbf{D}_{ij} = D_{ij}(\mathbf{r}_{ij} \times \mathbf{n})$ with constant D, describing DMI force in the film plane, where **n** — normal vector of the film interface. Therefore, interface DMI may be considered as equivalent of the effective flat magnetic field H_{DMI}, which, acting at the domain wall, causes reorientation of spins from Bloch configuration into Neel configuration with fixed chirality. At the same time the interface DMI value is measured in the experiment as DMI field [6,12]. Having defined the DMI field, within the so-called 1D model one can calculate the constant D in the HM/FM structure using formula [13,14]:

$$D = \mu_0 H_{\mathrm{DMI}} M_s \Delta, \qquad (2)$$

where M_s — saturation magnetization, H_{DMI} — field of Dzyaloshinskii–Moriya interaction, $\Delta = \mathrm{sqrt}(A_{\mathrm{ex}}/K_{\mathrm{eff}})$ — parameter corresponding to the width of the domain wall, where A_{ex} — constant of exchange interaction, $K_{\mathrm{eff}} = K_U - (\mu_0 M_s^2)/2$ — constant of effective anisotropy, defined as difference between the constant of perpendicular anisotropy K_U and demagnetization energy $(\mu_0 M_s^2)/2$.

For experimental definition of DMI field in planar structures of HM/FM type of small linear size, the classic experiment of slow neutron diffraction is poorly applicable (for example, method based on interference of non-resonant magnetic and resonant quadrupole scattering [15]), and such methods as [13,14,16,17] are often used:

1. Method of domain walls, where value and sign D are defined by direct measurement of domain wall motion speed depending on the magnetic field in the plane of the specimen, or by measurement of the field of origination of the reoriented domain depending on the value of the external magnetic field in the film plane etc.

2. Spin-wave method, where value and sign D are received by analysis of asymmetric dispersion of spin waves in nanoscale thin-film structures, relative to the magnetized ones in the plane, for example, using data of Brillouin light scattering, time-resolved Kerr spectroscopy etc.

3. Method of spin-orbit torque (SOT), where D is defined by measurement of value of current-induced effective field in the films with perpendicular magnetic anisotropy, depending on the current value and external magnetic field directed in the film plane.

The paper provides brief description of three methods of DMI field assessment: definition of the domain nucleation fields, registration of DW motion parameters and assessment of the value of the current-induced effective field. Using measurements of anomalous Hall effect and Kerr microscopy, experimental testing of methods was performed, and the assessment of Dzyaloshinskii–Moriya interaction for the synthesized multilayer nanostructure of Pt(4 nm)/Co(0.7)/MgO(2) composition with Hall contacts. Following the work results, the analysis of the used methods to assess the DMI field was performed, and the optimal approach was chosen.

2. Description of DMI calculation methods

2.1. Study of the dependence of the effective current-induced field on value of the external magnetic field in film plane

The method to determine efficiency of spin-orbit torque (SOT) and DMI field transfer in HM/FM film with perpendicular magnetic anisotropy is based on the model of current-induced distribution of domain wall [18,19]. Direct current I_{DC}, flowing in HM/FM structure with strong spin-orbit interaction in direction x due to spin-Hall effect or inverse spin galvanic effect creates a non-equilibrium density of spin states $\boldsymbol{\delta}$ in the transverse direction y. As a result, effective magnetic field arises, which acts at the magnetization of structure as $\mathbf{H}_{\mathrm{eff}} = \boldsymbol{\delta}\mathbf{M}$. As shown in Figure 2, *a*, Neel DW, apart from DMI field will be exposed to transverse vertical component of the field H_{eff}^z, which generally depends on the angle between the DW magnetization and direction of current density $\mathbf{J}_e$. However, for homochiral DW the total value of the effective field will be equal to zero due to opposite signs H_{eff}^z for DWs, which have the opposite direction of magnetization.

In this case in the absence of the external field the field H_{eff}^z may act on DW and move the domain in any

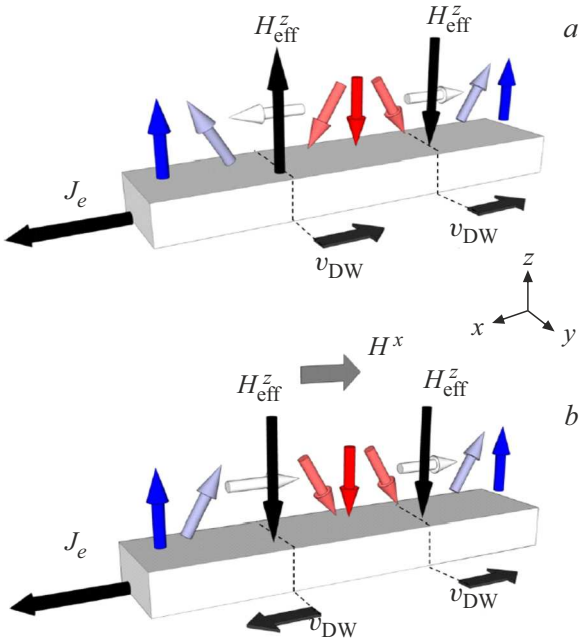

Figure 2. (*a*) Scheme of current-induced motion of DWs in magnetic film with PMA in absence of external magnetic field. Field H^z_{eff} is an effective field induced by the spin-Hall effect, acting on the Neel-type domain wall. $\mathbf{V}_{\text{DW}}$ represents a direction of DW motion, J_e — current density; (*b*) Scheme of domain expansion in magnetic field H_x as a result of rearrangement of DW magnetic moments (Reprinted with permission from [19]).

direction without its expansion — current-induced motion. However, if a rather large magnetic field is applied in the $H_x > H_{\text{DMI}}$ film plane, magnetization in DW will be built in parallel as shown in Figure 2, *b*, and then the resulting H^z_{eff} will be directed in the same manner for both DWs. Accordingly, expansion or compression of domains will be observed depending on the polarity of field H_x and current I_{DC}. Therefore, there is a direct interrelation between DW motion, perpendicular field H^z_{eff} and current value J_e and field H_x — $H^z_{\text{eff}}(J_e, H_x)$. Therefore, measuring the shift of magnetic loops of the nanostructure as a function $f(H_x, I_{\text{DC}})$, and knowing the saturation field of H_{sat} loop, it is possible to determine value $H_{\text{DMI}} = H_{\text{sat}}$.

As an example, paper [19] measured curves (loops) of anomalous Hall effect (AHE) dependence on perpendicular field V under variation of value and polarity of current I_{DC} and field H_x. It was shown that in field $H_x = 0.25\,\text{T}$ the transverse loop of AHE hysteresis moves to the opposite sides due to SOT effect for $I_{\text{DC}} = \pm 6\,\text{mA}$, which indicates the opposite sign of the induced effective field H^z_{eff}. Since H^z_{eff} acts as the effective magnetic field for the entire HM/FM structure, the AHE loop should move relative to the initial position at $H^z_{\text{eff}} = 0$ by value equal to H^z_{eff} [19]. Accordingly, measuring the shift of AHE hysteresis loop depending on H_x and I_{DC}, may obtain the dependence of type $H^z_{\text{eff}} = \chi I_{\text{DC}}$, where χ — indicator of efficiency of „charge–spin“ (SOT) transformation. Further, if J is fixed, one can define the value of DW switching fields: H^1_{SW} (up-down) and H^2_{SW} (down-up). Then, if the Joule heating (under small currents) and coercive field effect are excluded, the effective field H^z_{eff} may be defined as follows: $H^z_{\text{eff}} = (H^1_{\text{SW}} + H^2_{\text{SW}})/2$. In this case the critical value of field H_x, when the dependence of type $\chi(H_x) = dH^z_{\text{eff}}/dJ_e$ reaches plateau (saturation state, when DW magnetization is leveled by field H_x), will correspond to DMI field — $H_{\text{DMI}} = H_x$. Further, using equation (2), D is defined. Note that sign D is not defined from these measurements.

It is also important that the region of saturation of curve $\chi(H_x)$, where $\chi_s = H^z_{\text{eff}}(H_{\text{sat}}, J_e)/J_e$, may be used to assess the efficiency of the „charge–spin“ (SOT) transformation process in HM/FM nanostructures, which is important for practical applications [17–19].

2.2. Domain wall method

2.2.1 Study of dependence of domain nucleation field on field value in film plane

As described in paper [20], within the finite temperature model, remagnetization in the macroscopic specimen is carried out via origination of reoriented domains with subsequent motion of DWs and change in the domain size. Besides, the presence of DMI causes reduction of DW energy in the film structure, and also effects (reduces) the energy barrier necessary to form an origination center (droplet) of reoriented domains. At the same time, in [21] it was found a difference between the conditions of domain formation at the edge and in the center of the magnetic film and showed that occurrence of domains at the edge does not only depend on the field value H_x, but has asymmetry relative to the combination of DMI sign and field direction in the plane. At the same time the direction of domain origination center magnetization usually matches the direction of the applied external magnetic field. In [21,22], to describe the start of formation of the magnetic domain at the edge of the film under the magnetic field effect, a „half-droplet“ model was used. According to the model, the field of origination of the reoriented domain, H_n at the edge of the film with PMA is determined by the Zeeman energy and full energy of DW (σ):

$$H_n = \frac{\pi\sigma^2 t}{2\mu_0 M_s p k_{\text{B}} T}, \tag{3}$$

where t — FM layer thickness, p — thermal stability factor related to the time of activation of reoriented domains $\tau = \tau_0 e^p$, where τ_0 — reverse frequency of origination attempts, μ_0 — constant of magnetic susceptibility, M_s — saturation magnetization, k_{B} — Boltzmann's constant, T — temperature.

From equation (3) it follows that the field of origination is proportionate to the square of DW full energy, which in its turn depends on DMI value and external magnetic field H_x applied in the film plane [23]. However, this model may not be applied to description of domain origination

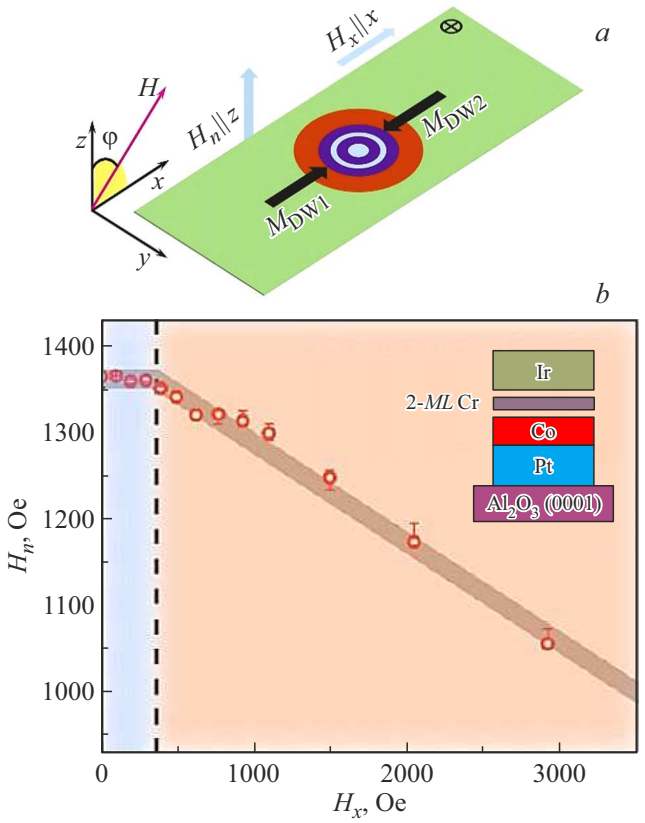

Figure 3. (a) Schematic image of domain nucleation center in film with PMA with opposite directions of magnetization marked with red and blue regions. DW magnetization (M_{DW1}, M_{DW2}) is shown by arrows in the plane. (b) Dependence of the nucleation field H_n on the external field in the plane of film H_x for Pt/Co/Ir nanostructure, where the blue region notes experimental points at $H_x < H_{DMI}$, and the orange region corresponds to half-interval $H_x > H_{DMI}$ ($H_x^c = 409$ Oe) [Reprinted with permission from [23] Copyright {2024} ACS].

in case when value of field H_x exceeds certain critical value H_c, corresponding to DMI field. This happens due to the match in the directions of domain boundaries magnetization directions with field direction in the plane, which causes reduction of magnetic energy of the origination center and, accordingly, reduction of the nucleation field value at $H_x^c > H_{DMI}$. Therefore, value H_x^c, under which the field of origination starts depending on field H_x, presents a „comparability indicator" of the nucleation field with field H_{DMI}. This parameter may be determined experimentally from the analysis of curve $H_n(H_x)$ behavior.

This method is successfully used in the studies of domain structure and DMI assessment in multilayer nanostructures with PMA [20–23]. At the same time, to control/determine nucleation field, Kerr microscopy (MOKE) may be used, for example. The scheme of magnetic nucleus (droplet) and device with Hall contacts is shown in Figure 3, a. The total energy of domain wall σ is defined as the sum of surface energy for each of them related to magnetization of DW. These directions are parallel and antiparallel to the external field H_x, which is shown by arrows in Figure 3. Value σ remains invariable provided that $H_x < H_{DMI}$ and decreases at $H_x > H_{DMI}$. For example, dependence $H_n(H_x)$ has a plateau in the interval of $0 < H_x < H_{DMI}$ and finds dramatic deviation (reduction of value H_n) in case of $H_x > H_{DMI}$ (Figure 3, b) [23]. According to model [23], the critical value of field H_x^c, when curve $H_n(H_x)$ demonstrates a kink, determines the value of field H_{DMI} in the film. Therefore, from experimental dependence $H_n(H_x)$ one can assess DMI field and value D.

2.2.2 Study of dependence of domain motion speed on field value in plane

Contactless methods of DMI assessment in magnetic nanostructures with PMA include analysis of DW motion in fixed perpendicular magnetic field H_z under simultaneous exposure to the field in plane H_x using Kerr microscopy. It is assumed that to minimize Zeeman energy related to H_z, domains with magnetization along direction of field H_x expand due to the domains of other orientations, which causes DW motion. DW dynamics is usually considered as the motion of unidimensional elastic line in 2D disordered potential. Besides, three motion modes are identified: „creep", „depinning" and „flow" which occur in parallel with increase of field H_z [24]. At rather weak fields, DWs move in the mode of thermally assisted creep. In this case they interact strongly with fluctuations of various origin, including thermally assisted ones, and DW speed varies as $v \sim \exp(-H_x)^{-1/4}$. As H_z increases to critical value, equal to depinning field H_{dep}, the effect of thermal fluctuations weakens, and DW speed rises as $v \sim (H_x - H_{dep})^{\beta}$, where β is the indicator of depinning degree at $T = 0$ [24]. Finally, at $H_x > H_{dep}$ the domain wall achieves „span mode", at which the speed of its motion increases linearly to Walker breakdown and further dramatically drops due to the change in the internal magnetic structure of DW [25].

In the experiments the value H_{DMI} most often is determined by DW motion in the permanent perpendicular field H_z in the creep mode. In this mode DWs move slowly in weak fields (several percents of H_{dep}) due to thermal activation, interacting with defects of various origin (pinning defects, changes of film thickness, magnetic and structural irregularities etc.) [24,25]. DW motion speed under perpendicular field substantially varies in the presence of the field in the plane (H_x). Besides, in this case the domain should grow isotropically, maintaining the initial radial-symmetric shape. Experimentally it manifests itself as magnetic domain expansion. However, in the presence of directed field H_x the symmetry of the expanding domain is affected, since Neel DWs on the opposite edges of the domain have the oppositely directed planar component of magnetization and, accordingly, acquire various speeds under action of field H_x [26]. Asymmetric growth of the domain is registered using Kerr microscopy [27–29]. Depending on the value of field H_x and method of

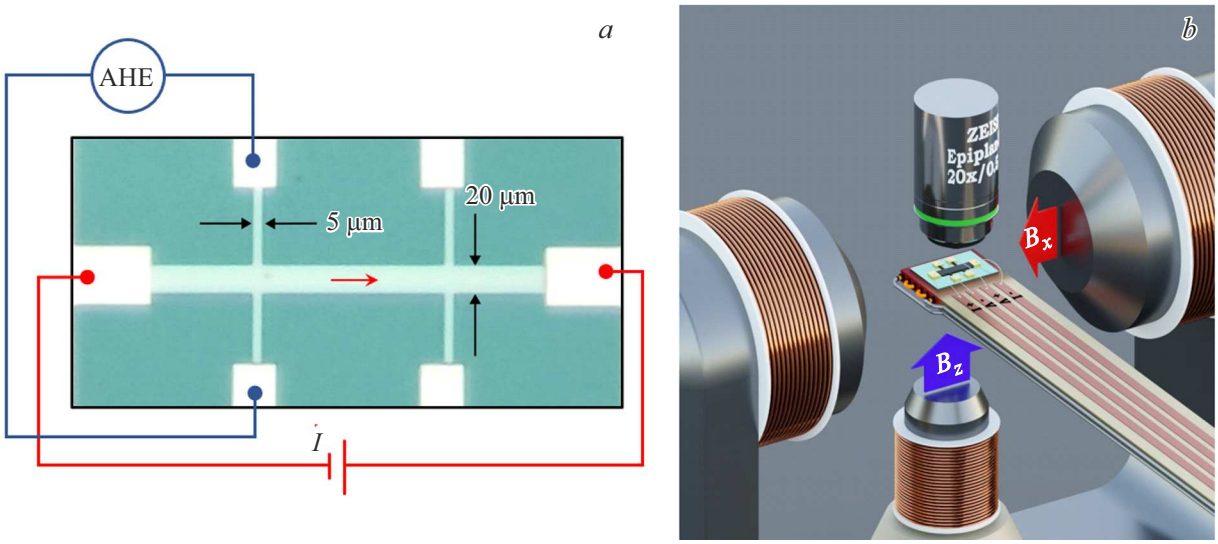

Figure 4. (*a*) Specimen of studied films with Hall structure, (*b*) Schematic image of experimental installation with Kerr microscope equipped with assembly of electromagnets to develop orthogonal fields.

application of field H_z, using the domain shape and size, the DW motion speed is calculated, and its dependence $v(H_x)$ is plotted. In the case when the external field H_x becomes equal to DMI field, the internal magnetic structure of DW changes — transition from Neel wall to Bloch wall, which is accompanied by the minimum on the curve of domain wall motion speed dependence $v(H_x)$. Accordingly, the DMI field value is usually field H_x, corresponding to this minimum. DMI value is determined using equation (2), and its sign — by orientation of domain asymmetry relative to direction H_x. The modified „creep" model, where the external magnetic field in the film plane affects the dynamics of the domain only by measurement of DW energy, is successfully used for analysis of experimental data and assessment of DMI constant in various rather lengthy metal thin-film nanostructures with PMA. Note that in the considered model the speeds of opposite DWs should be symmetrical with respect to zero. However, in multiple experimental cases it is not so: the produced dependences $v(H_x)$ are often asymmetric and/or have the shape different from parabola [31,32]. In such cases the model and calculations become very complicated.

See above the description of three methods to determine DMI value in magnetic films. In the next section, to compare each of the proposed models, the experimental determination of DMI field was performed in the specimens of thin-film nanoheterostructure of heavy metal/ferromagnetic.

3. Comparison of experimental results of DMI value determination

For experiments, the test specimens used were thin-film nanostructures with composition of Pt(4)/Co(0.7)/MgO(2 nm), deposited on the surface of the oxidized silicon. Hall structures and contact sites were formed on the produced films by methods of photolithography and ion-plasma etching (Figure 4, *a*). You can review the methods of synthesis and certification of films and preparation of contents in more detail, for example, in [33,34].

In the first method the experiment studied the dependence of the effective current-induced magnetic field H_{eff}^z on the value of the external magnetic field. For this purpose, a film with Hall structure was used, which was placed in Kerr microscope, equipped with two electromagnets, making it possible to simultaneously develop horizontal and vertical fields (in the plane and perpendicularly to the plane of the specimen) (Figure 4, *b*). In the experiment the specimen was remagnetized by vertical field H_z, and the anomalous Hall effect (AHE) hysteresis loop was measured at the same time. Further, direct current of difference signs ± 5 mA was passed through the specimen in the presence of the permanent horizontal magnetic field H_x. Current generates effective magnetic field H_{eff}^z, perpendicular to field H_x. Direction of field H_{eff}^z depends on current polarity. As a result, the AHE hysteresis loop will move relative to its start position to the left or to the right, by the value proportionate to the value of the current-induced field H_{eff}^z (Figure 5, *a*).

In the experiment the value of the shift field H_{sw} was obtained for the values of magnetic field H_x in the interval from -30 to 30 mT with increment 2.5 mT. The resulting dependence $H_{sw}(H_x)$ is shown in Figure 5, *b*. In accordance with the theory described above , the value of field H_x was determined using the produced experimental data, at which the curve reaches saturation. For the used specimen of nanostructure, this value was 16 mT, which agrees with the estimates of DMI field for Pt/Co/MgO structures obtained in [31,32].

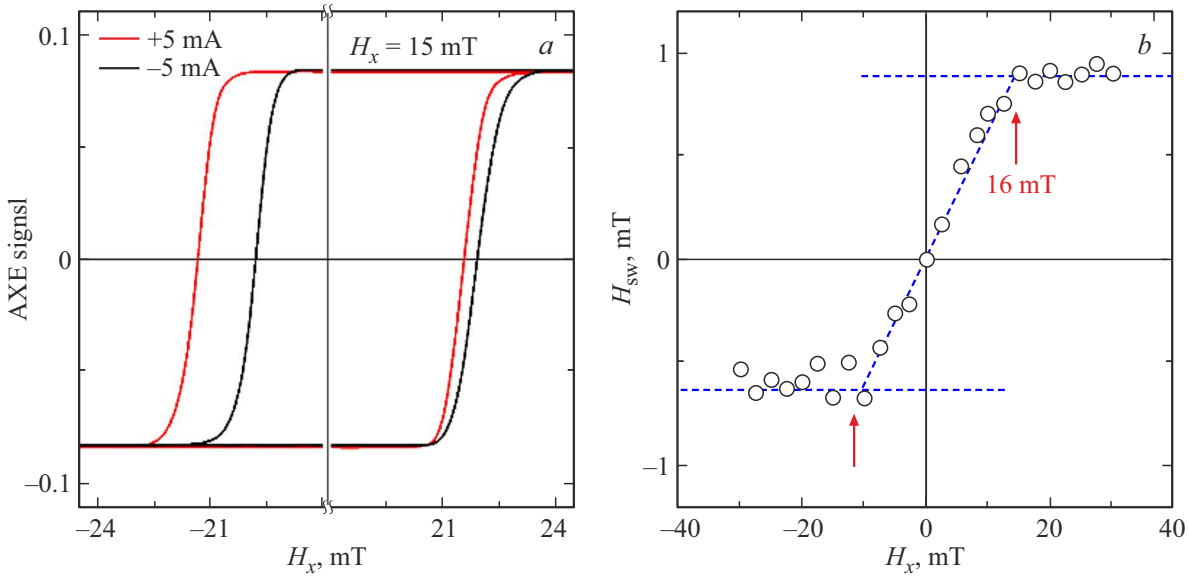

Figure 5. (*a*) Shift of anomalous Hall effect (AHE) hysteresis loops produced by structure remagnetization depending on current polarity in horizontal field H_x. (*b*) Dependence of hysteresis loop shift value H_{sw} on field value in plane H_x. In each case, current ±5 mA was used to determine the shift.

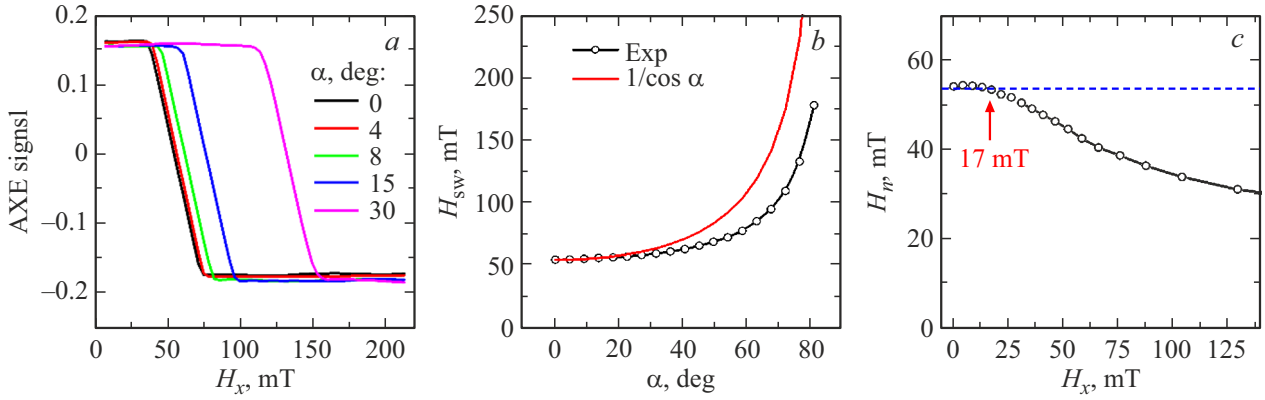

Figure 6. (*a*) Anomalous Hall effect (AHE) hysteresis half-loop obtained at various angles of specimen orientation relative to external field H_x, (*b*) Dependence of magnetization switching field H_{SW} on angle α between field direction and specimen plane. The solid red line corresponds to the theoretical case of invariable nucleation field, (*c*) Dependence of the domain nucleation field H_n on value of external magnetic field component in film plane H_x.

Further, the dependence of domain nucleation field H_n on angle α between the specimen plane and the direction of the external magnetic field H_x was studied using the same specimens. Note that for such modified method the development of two orthogonal fields is not required. In the experiment the film with a Hall structure was fixed on the rotary holder between the poles of the electromagnet, which could rotate thanks to a step motor with an increment of 1 degree. In this case at $\alpha = 0$ degrees field H_x is oriented perpendicularly to the plane of the specimen, and at $\alpha = 90$ degrees — in the plane. Therefore, deviation of the holder from 0 degrees results in the fact that the external magnetic field H_x starts having two non-zero projections relative to the specimen plane: $H_{xy} = H_x \sin\alpha$ and $H_{xx} = H_x \cos\alpha$. For each value of the holder angle, an AHE hysteresis loop was recorded under variation of field H_x, and the value of the switching field H_{sw} was determined. As angle α increased, the field H_{sw}, which is necessary to switch the orientation of magnetization, increased, and the loop, accordingly, expanded (Figure 6). Based on experimental data a dependence was built of $H_{SW} = H_{SW}(0^0)\cos\alpha$ type, which is approximated well by a curve of $1/\cos\alpha$ type, describing the process of remagnetization in the Kondorsky model and fair in the case when the domain nucleation field in the film does not depend on the value H_x. Further, according to equations $H_x = H_{sw}(\alpha)\sin\alpha$ and $H_n = H_{sw}(\alpha)\cos\alpha$ the dependence $H_n(H_x)$ was built, corresponding to the field of domain

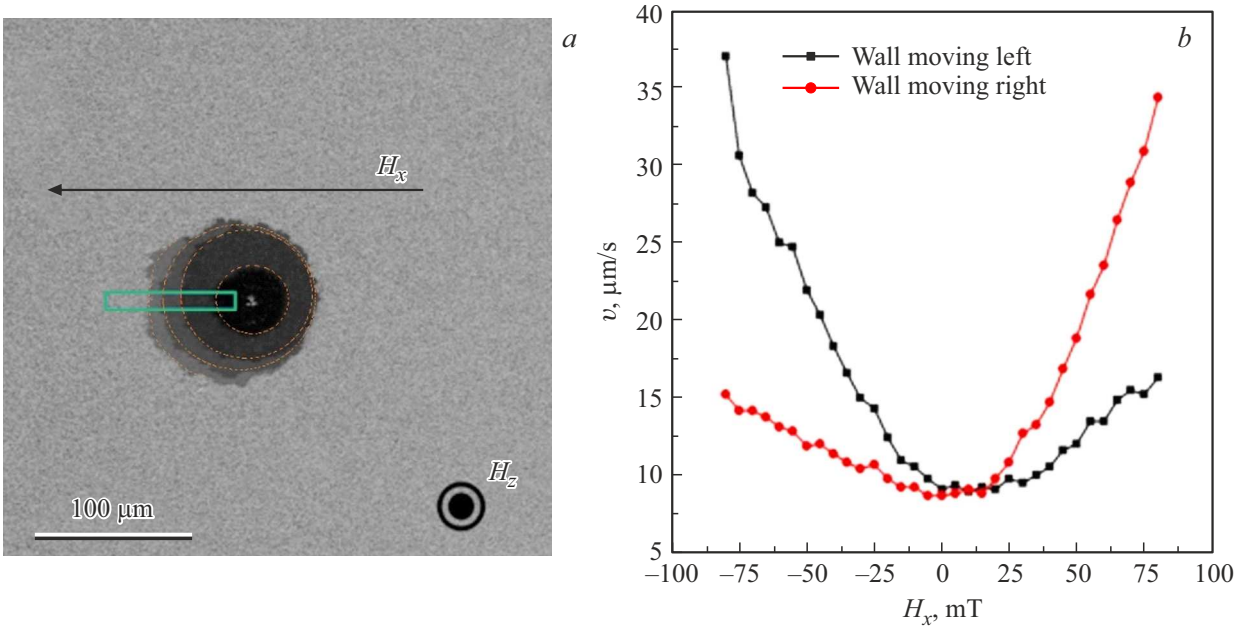

Figure 7. (*a*) Example of growth (shift) of domain exposed to impulses of vertical field $H_z = 50$ mT in presence of horizontal field $H_x = 50$ mT (the scale is shown in the lower left corner. The color frame highlights the DW motion area). (*b*) Dependences of motion speed of the left and right DW (v) in nanostructure on external magnetic field H_x.

switching, on the component of the external magnetic field in the film plane (Figure 6, *c*). According to section 2.2.1, the field, under which this dependence deviates from the permanent value (saturation state), corresponds to DMI field. Therefore, in the considered case this value was 17 mT, which agrees with the data obtained by the first method, and complies with the DMI field for such structures [33–35].

In the third method the same films were used to study the dependence of the DW motion speed on the field value in the specimen plane H_x. For the experiment, a magnetooptical installation was used, the image of which is shown in Figure 4, *b*. First, using Kerr microscope, a center of origination was found, where the external vertical field H_z led to remagnetization of the film accompanied by the process of symmetric domain growth. To determine the DW motion speed, the domain size was first minimized by selection of the value and sign of field H_z. After that three pulses of field H_z with duration of around 10 ms were fed to the specimen. After each pulse, the photo of the magnetic structure of the film was saved (Figure 7, *a*). Then, based on the received exposures, the average motion speed was estimated for the left and right DW (Figure 7, *b*). The measurements were made for the fixed values of field H_x from -0.1 to $+0.1$ T with increment 0.01 T. In accordance with the theory described in section 2.2.2, the field, under which the obtained dependences achieve the minimum, was taken as DMI field.

In the considered case the DMI field made around 17 mT for the right DW and around 1–2 mT for the left DW. Asymmetry of dependences $v(H_x)$ is possibly related to the defectiveness of the film, heterogeneity and instability of magnetic fluxes H_x and H_z, thermal fluctuations in the film as a result of heterogeneous heating etc. Therefore, compared to the method for assessment of the nucleation field this method is more demanding to the quality of the specimen, level of the experimenter and the level of the experimental set up, i. e. higher error of DMI determination.

Based on the analysis of the theoretical models of DMI assessment and the conducted experiments one can conclude that the first method (current-induced DW shift) is direct and adequate method for DMI assessment (except for sign) without involvement of complex mathematical models. The method is applicable even for nanoscale films, but the specimens must have PMA and the most symmetric AHE loop. Note the need for involvement of complex lithographic processes to make Hall structures. Besides, this method requires quadrupole configuration of magnets, higher density and higher homogeneity of orthogonal magnetic fields, which is technically costly. Thus, the second method (assessment of the nucleation field) with the similar technique and precision of the experiment requires only one source of the external magnetic field, optical Kerr microscope and a simple device to rotate the specimen in the magnetic field. The third method (measurement of DW motion) is demanding to the defectiveness of the ultrathin film specimens, and also to precise compliance with the condition for one of three DW shift modes, which is an individual parameter for each specimen. Besides, the technical implementation of Kerr microscopy and implementation of strict orientation and value of the field for the specific shift mode require certain level of ex-

perimenter training and compact precise stabilized sources of magnetic field. According to formula (2), all methods also require the accurate value of saturation magnetization and exchange hardness (DW width), definition of which for nanoscale structures is a separate complicated experimental task. This results in the fact that the error of DMI field and constant D determination for the described methods is usually around 30%. Besides, all considered methods are naturally limited by the maximum field value in the plane, which somewhat limits the range of the measured DMI values.

Therefore, the most universal approach would be the complex measurement of DMI with methods that supplement each other and are based on different physical phenomena, for example: domain wall motion method and spin-wave method. Among the considered approaches for DMI assessment, the method to determine dependence of the nucleation field on the external magnetic field from the AHE loop analysis data seems to be the fastest and least labor-intensive.

To conclude, one can also note that the spread in the DMI values in the literature even for the specimens of nanostructures of formally one and the same type and composition is first of all defined by not only and not that much the measurement method, but by the individual material parameters (for example, roughness and homogeneity of the layers and interfaces, epitaxial stresses etc.) of the specimens, therefore the performance of the complex of experiments on one and the same specimen will be the most effective approach and undoubted advantage of any experimental work on this subject.

4. Conclusion

The paper describes the main methods used to assess the Dzyaloshinskii–Moriya interaction based on domain wall motion in thin-film magnetic structures, and the experimental analysis of these methods was performed for multilayer metal films Pt(4)/Co(0.7)/MgO(2 nm). It was shown that the methods to assess the nucleation field or the value of the current-induced field provide a good match in the assessment of the Dzyaloshinskii–Moriya interaction field with good reproduction. However, for these methods it is necessary to create nanostructures with Hall contacts, which requires using a complex photolithographic process, development of contact sites and performance of precision electrical measurements. The method to assess the domain wall motion speed with the help of Kerr microscopy under the external magnetic field is also technically complex and demanding to both quality and thickness of the film itself and the level of experiment set up, experimenter's skills and many other hard-to-account-for factors, which causes large spreads of final estimates.

Based on the comparison of model approaches and experimental data, the conclusion was made on the fact that the simplest method for implementation and calculations is the method to assess the domain nucleation field upon specimen remagnetization in inclined fields. From our point of view, it may be recommended as a complementary to one of the current most common contactless spin-wave methods of Dzyaloshinskii–Moriya interaction assessment in nanostructures using Brillouin light scattering.

Acknowledgments

The authors thank Doctor of Physical and Mathematical Sciences Yu.P. Sukhorukov (Institute of Metal Physics, Ural Branch of the Russian Academy of Sciences).

Funding

This study was supported by grant No. 21-72-20160 from the Russian Science Foundation (https://rscf.ru/en/project/21-72-20160).

Conflict of interest

The authors declare that they have no conflict of interest.

References

[1] A. Fert, UFN **178**, *12*, 1336 (2008). (in Russian).
[2] A. Fert, F.N. Van Dau. Comptes Rendus Physique **20**, *7–8*, P. 817 (2019).
[3] K. Everschor-Sitte, J. Masell, R.M. Reeve, M. Kläui. J. Appl. Phys. **124**, *24* (2018).
[4] I. Dzyaloshinsky. Sov. Phys. JETP **5**, 1259 (1957); T. Moriya. Phys. Rev. Lett. **4**, 228 (1960).
[5] R.E. Camley, K.L. Livesey. Surface Science Reports **78**, *3*, 100605. (2023).
[6] W.S. Wei, Z.D. He, Z. Qu, H.F. Du. Rare Metals **40**, *11*, 3076 (2021).
[7] B. Göbel, I. Mertig, O.A. Tretiakov. Physics Reports **895**, 1 (2021).
[8] A.N. Bogdanov, C. Panagopoulos. Nat. Rev. Phys. **2**, *9*, 492 (2020).
[9] B. Kaviraj, J. Sinha. ECS Journal of Solid State Science and Technology **11**, *11*, 115003 (2022).
[10] M. Ma, Z. Pan, F. Ma. J. Appl. Phys., **132**, *4*, 043906 (2022).
[11] A.S. Samardak, A.G. Kolesnikov, A.V. Davydenko, M.E. Stebliі, A.V. Ognev. Phys. Met. Metallogr. **123**, 238 (2022).
[12] A. Thiaville, S. Rohart, É. Jué, V. Cros, A. Fert. Europhysics Letters **100**, *5*, 57002 (2012).
[13] M. Kataoka. J. Phys. Soc. Jpn. **56**, 3635 (1987).
[14] S. Emori, U. Bauer, S.M. Ahn, E. Martinez, Geoffrey S.D. Beach. Nat. Mater. **12**, 611 (2013).
[15] V.E. Dmitrienko, E.N. Ovchinnikova, S.P. Collins, G. Nisbet, G. Beutier, O. Kvashnin, V.V. Mazurenko, A.I. Lichtenstein, M.I. Katsnelson. Nature Physics **10**, 202 (2014).
[16] M. Bode, M. Heide, K. von Bergmann, P. Ferriani, R. Wiesendanger. Nature **447**, *7141*, 190 (2007).
[17] A. Manchon, J. Zelezny, I.M. Miron, T. Jungwirth, P. Gambardella. Rev. Mod. Phys. **91**, *3*, 035004 (2019).
[18] Y. Ishikuro, M. Kawaguchi, M. Hayashi. Phys. Rev. B **99**, *13*, 134421 (2019).

[19] C.F. Pai, M. Mann, Aik Jun Tan, G.S.D. Beach. Phys. Rev. B. **93**, *14*, 144409 (2016).
[20] S. Pizzini, J. Vogel, S. Rohart, L.D. Buda-Prejbeanu, E. Jue, O. Boulle, I.M. Miron, C.K. Safeer, S. Auffret, G. Gaudin, A. Thiaville. Phys. Rev. Lett. **113**, *4*, 047203 (2014).
[21] J. Vogel, J. Moritz, O. Fruchart, C.R. Physique **7**, *9–10*, 977 (2006).
[22] S. Kim, P.-H. Jang, D.-H. Kim, M. Ishibashi, T. Taniguchi, T. Moriyama, K.-J. Kim, K.-J. Lee, T. Ono. Phys. Rev. B **95**, *22*, 220402 (2017).
[23] J. Qi, Y. Zhao, H. Huang, Y. Zhang, H. Lyu, G. Yang, J. Zhang, B. Shao, K. Jin. Y. Zhang, H. Wei, B. Shen, S. Wang. J. Phys. Chem. Lett. **14**, *3*, 637 (2023).
[24] P. Chauve, T. Giamarchi, P. Le Doussal. Phys. Rev. B **62**, 6241 (2000).
[25] P.J. Metaxa, J.P. Jamet, A. Mougin, M. Cormier, J. Ferre, V. Baltz, B. Rodmacq, B. Dieny, R.L. Stamps. Phys. Rev. Lett. **99**, 217208. (2007).
[26] Y.P. Kabanov, Y.L. Iunin, V.I. Nikitenko, A.J. Shapiro, R.D. Shull, L.Y. Zhu, C.L. Chien. IEEE Trans. Magn. **46**, *6*, 2220 (2010).
[27] R.A. Khan, P.M. Shepley, A. Hrabec, A.W.J. Wells, B. Ocker, C.H. Marrows, T.A. Moore. Appl. Phys. Lett. **109**, *13*, 132404 (2016).
[28] K. Grochot, P. Ogrodnik, J. Mojsiejuk, P. Mazalski, U. Guzowska, W. Skowroński, T. Stobiecki. Sci. Rep. **14**, 9938 (2024).
[29] M. Kuepferling, A. Casiraghi, G. Soares, G. Durin, F. Garcia-Sanchez, L. Chen, C.H. Back, C.H. Marrows, S. Tacchi, G. Carlotti. Rev. Mod. Phys. **95**, *1*, 015003 (2023).
[30] A. Hrabec, N.A. Porter, A. Wells, M.J. Benitez, G. Burnell, S. McVitie, D. McGrouther, T.A. Moore, C.H. Marrows. Physical Review B. **90**, *2*, 020402 (2014).
[31] S.G. Je, D.H. Kim, S.C. Yoo, B.C. Min, K.J. Lee, S.B. Choe. Phys. Rev. B **88**, *21*, 214401 (2013).
[32] K. Richter, R. Varga. Acta Physica Polonica A **137**, *5*, 741 (2020).
[33] A.S. Samardak, A.V. Davydenko, A.G. Kolesnikov, A.Y. Samardak, A.G. Kozlov, B. Pal, A.V. Ognev, A.V. Sadovnikov, S.A. Nikitov, A.V. Gerasimenko, I.H. Cha, Y.J. Kim, G.W. Kim, O.A. Tretiakov, Y.K. Kim. NPG Asia Materials **12**, *1*, 51 (2020).
[34] A.V. Telegin, Z.Z. Namsarasev, V.D. Bessonov, V.S. Teplov, A.V. Ognev. Mod. Electr. Mat. **10**, *1*, 51 (2024).

Translated by M.Verenikina